

Absolute Intensities of Nitric Acid Overtones

D. J. Donaldson*

Department of Chemistry and Scarborough College, University of Toronto, Toronto, Ontario, Canada M5S 1A1

J. J. Orlando, S. Amann, and G. S. Tyndall

National Center for Atmospheric Research, Boulder, Colorado 80307

R. J. Proos and B. R. Henry

Department of Chemistry and Biochemistry, University of Guelph, Guelph, Ontario, Canada N1G 2W1

V. Vaida

Department of Chemistry and Biochemistry, University of Colorado, Boulder, Colorado 80309-0215

Received: January 16, 1998; In Final Form: April 28, 1998

The absolute absorption cross sections for the $\Delta v = 3$ and $\Delta v = 4$ OH local mode transitions in room-temperature, gas-phase nitric acid have been measured and calculated ab initio. The measured [calculated at the QCISD/6-31+G(d,p) level] oscillator strengths are $(2.9 \pm 0.3) \times 10^{-8}$ [2.78×10^{-8}] and $(2.7 \pm 0.3) \times 10^{-9}$ [2.14×10^{-9}]. Scaling the calculated values by 1.15 (the average ratio of *measured:calculated*) yields predicted oscillator strengths for transitions to $v = 5$ and $v = 6$ of 2.9×10^{-10} and 4.0×10^{-11} , respectively, corresponding to integrated absorption cross sections of 2.6×10^{-22} and 3.5×10^{-23} cm² molecule⁻¹ cm⁻¹, respectively for these transitions. These values are almost 2 times larger than previously estimated.

Introduction

Overtone excitation of X–H (X = C, N, O) oscillators has been used extensively to prepare molecules in initial states with energy localized in the X–H bond. Because of the high frequency and anharmonicity of typical X–H stretches, they become decoupled from the molecular normal modes at fairly low energies (corresponding to 2–3 quanta in the stretch) and become well described by local mode basis sets.^{1,2} These local mode overtones appear in the visible region of the spectrum and so are easily accessible by intense dye lasers. Molecules have been prepared in X–H overtone states to study intramolecular energy distribution (IVR)³ and overtone-initiated ground electronic state dissociation,⁴ to prepare a wave packet for projection to a dissociative excited electronic state,⁴ and to “label” a specific bond in a molecule for bimolecular reaction.⁴

The calculation of the energies and intensities of X–H local mode overtone transitions provides a sensitive test for theory. In general, there is a “chemical transferability” to both the frequencies and intensities.^{5,6} Overtone intensities decrease approximately exponentially as a function of the vibrational quantum number.⁷ Accurate calculation of the intensities demands accurate vibrational wave functions and knowledge of the dipole moment function to high order; both require accurate potential energy calculations, especially of the inner wall of the potential describing the local mode.⁶

Vibrational overtones of atmospherically important molecules are accessible in the visible region of the spectrum, where high fluxes of solar photons are available. Some of us⁸ have recently shown by way of an atmospheric model that solar pumping of vibrational overtones of H₂O₂, HNO₃, and HNO₄ provides a significant source of OH at dusk and dawn and on the edge of the polar vortex where near-UV radiation is not available but

visible light is significant. These findings underscore the need for quantitative understanding of the factors that determine absorption cross sections of vibrational overtones at chemically relevant energies.

Nitric acid, HNO₃, has been used as a prototype molecule in studies of IVR and dissociation following H–ONO₂ overtone excitation.^{9,10} Dissociation to OH + NO₂ is energetically allowed (and takes place) following excitation to $v = 6$ of the H–O stretch, as well as higher thermally populated rotational levels in $v = 5$. Recently, this process, taking place in the visible region of the spectrum between about 500 and 620 nm, was postulated⁸ to account for some of the sudden burst of HO_x and NO_x observed¹¹ at 15 km altitude at sunrise. The major uncertainty in that postulate was the fact that the values of the absorption intensities into the H–O overtone bands were unknown, to within an order of magnitude. In the following, we present the results of quantitative spectroscopic measurements and ab initio calculations of these absorption strengths. In conjunction, these studies allow the prediction of O–H overtone intensities at chemically relevant energies.

Experimental Section

Absorption measurements were made in an apparatus described previously.¹² A 100 cm path length Pyrex cell, outfitted with 1.5 in. diameter quartz windows, was filled with various pressures from 2 to 12 Torr of neat nitric acid from a (almost) metal-free gas handling system. The pressure was measured using a 10 Torr capacitance manometer. Nitric acid was distilled from a mixture of 65% HNO₃ in concentrated H₂SO₄ immediately prior to use.¹³ This preparation yields <1% H₂O impurity, as measured by FTIR absorption.¹³ No other OH-containing species were detected. A trace (10–20 mTorr) of

TABLE 1: Calculated Equilibrium Geometry at Various Levels of Theory (Distances in Å and Angles in deg)

	r_{HO_1}	r_{NO_1}	r_{NO_2}	r_{NO_3}	$\angle\text{HO}_1\text{N}$	$\angle\text{O}_1\text{NO}_2$	$\angle\text{O}_1\text{NO}_3$
experimental ^a	0.964 ± .01	1.406 ± .01	1.211 ± .01	1.199 ± .01	102.2 ± 1.0	115.9 ± 1.0	113.8 ± 1.0
HF/6-31G(d)	0.9549	1.3337	1.1878	1.1723	105.33	116.05	114.79
HF/6-31+G(d,p)	0.9516	1.3330	1.1892	1.1727	105.74	116.07	114.92
HF/6-311+G(d,p)	0.9491	1.3331	1.1825	1.1650	105.75	116.12	114.84
HF/6-311++G(3df,3pd)	0.9480	1.3293	1.1801	1.1634	105.40	116.06	114.86
MP2/6-31G(d)	0.9829	1.4116	1.2262	1.2160	102.13	115.75	113.64
MP2/6-31+G(d,p)	0.9763	1.4151	1.2276	1.2167	102.65	115.85	113.62
MP2/6-311+G(d,p)	0.9708	1.4106	1.2140	1.2031	102.70	115.82	113.63
QCISD/6-31G(d)	0.9796	1.3946	1.2211	1.2058	102.62	115.76	114.07
QCISD/6-31+G(d,p)	0.9733	1.4027	1.2231	1.2067	103.10	115.81	114.02

^a From ref 24.

NO_2 is always present due to nitric acid decomposition on the walls of the apparatus. This does not cause any interference in the $\nu = 3, 4$ OH overtone region measured here but prevents a quantitative measurement of the $\nu = 5$ region (vide infra).

The output of a quartz-halogen lamp was collimated and passed through the cell; the transmitted light was focused onto the entrance slit of a 0.3 m Czerny-Turner monochromator, dispersed, and imaged onto a cooled diode array detector. The estimated spectral resolution of the system is 0.6 nm. The diode array output was averaged and sent to a computer for analysis and storage. Several lines from a Hg lamp were used to calibrate the wavelength scale of the diode array. Absorption spectra were collected at 296 ± 2 K in several overlapping segments between 600 and 1020 nm and smoothed upon analysis. The smoothing resulted in a degradation of the spectral resolution, to about 1 nm.

Absorption cross sections were obtained from the measured absorbance, $A = \ln[I_0(\lambda)/I(\lambda)] = \sigma(\lambda)lc$, where σ represents the absorption cross section in $\text{cm}^2 \text{molecule}^{-1}$, l is the path length, and c gives the HNO_3 concentration in molecules cm^{-3} . For each point in the digitized spectrum, a plot was constructed of A/l vs c , the slope of which yields the absorption cross section for that wavelength. These plots were all linear with an intercept of zero, suggesting that nitric acid dimerization is not important under our measurement conditions.

Calculations

Overtone intensities were calculated as detailed in previous works.¹⁴ The oscillator strengths, $f_{g \rightarrow e}$, of vibrational overtone transitions from $|g\rangle$ to $|e\rangle$ are given by^{14,15}

$$f_{g \rightarrow e} = 4.70165 \times 10^{-7} [\text{cm D}^{-2}] \hat{\nu}_{\text{eg}} |\boldsymbol{\mu}_{\text{eg}}|^2$$

where $\hat{\nu}_{\text{eg}}$ gives the transition frequency in cm^{-1} and $\boldsymbol{\mu}_{\text{eg}}$ represents the transition dipole moment matrix element, $\langle e|\boldsymbol{\mu}|g\rangle$, in debye. We take the wave functions describing the OH stretch to be the eigenfunctions of a Morse oscillator whose Hamiltonian is

$$(H - E_{|0\rangle})/hc = \omega v - \omega x v(v + 1)$$

where $\omega = 3707 \text{ cm}^{-1}$ and $\omega x = 79 \text{ cm}^{-1}$, recalculated from the values given by Sinha et al.^{9a}

The dipole moment function is expressed as a seventh-order Taylor series expansion in the internal H-O bond length coordinate, q , expanded about the equilibrium position:

$$\boldsymbol{\mu}(q) = \sum \boldsymbol{\mu}_i q^i$$

where the coefficients $\boldsymbol{\mu}_i$ are given by

$$\boldsymbol{\mu}_i = \frac{1}{i!} \left. \frac{\partial^i \boldsymbol{\mu}}{\partial R^i} \right|_e$$

The coefficients in this expansion are obtained by stretching the H-O bond by $\pm 0.4 \text{ \AA}$ in increments of 0.1 \AA and calculating the dipole moment at each position using ab initio quantum calculations.¹⁶ Several basis sets and levels of theory were used in these calculations. The calculated equilibrium geometry at each level of calculation and the dipole derivatives at the MP2/6-311+G(d,p) level are presented in Tables 1 and 2, respectively.

Results and Discussion

Figure 1 illustrates the HNO_3 absorption spectrum measured from 750 to 990 nm. Absorption features are seen at 755, 845, 877, 883, 942, and 983 nm. The peaks at 755 and 983 nm are by far the strongest and correspond to the $\nu = 4$ and $\nu = 3$ OH stretch transitions, respectively. Repeated attempts to measure the $\nu = 5$ overtone did not yield quantitative results. The trace of NO_2 present in all HNO_3 samples gave rise to a structured absorption spectrum in the $\nu = 5$ region which precluded any accurate measurement of the overtone intensity. On the basis of the known¹⁷ NO_2 absorption cross sections in this wavelength region, we can set an upper limit of $1 \times 10^{-23} \text{ cm}^2 \text{molecule}^{-1}$ for the peak absorption cross section of the $\nu = 5$ overtone transition.

Table 3 gives the peak positions and our assignments, based on the vibrational frequencies given in McGraw et al.¹⁸ We tentatively assign the feature at (877–883 nm) to a combination band of OH stretch and the N-O-H bend ($3\nu_{\text{OH}} + \nu_{\text{bend}}$), about 20–50 times weaker than the pure $3\nu_{\text{OH}}$ band. Such a combination band has been reported in the region of $2\nu_{\text{OH}}$ in the liquid-phase spectrum.¹⁹ We assign the feature at 942 nm to a combination of OH stretching and torsion ($3\nu_{\text{OH}} + \nu_{\text{torsion}}$). The very small intensity in this band stands in contrast to the corresponding feature observed in the $6\nu_{\text{OH}}$ region of the H_2O_2 overtone spectrum,²⁰ which is about 10% as intense as the pure overtone band.

Figure 2 shows the $3\nu_{\text{OH}}$ and $4\nu_{\text{OH}}$ transitions on expanded scales. The resolution of the experiment (1 nm) is not sufficient to resolve the P,Q,R-branch structure in $\nu = 4$, seen in photoacoustic^{9a} and OH production spectra,^{9a,10} but is just sufficient to do so in the $\nu = 3$ band. The integrated areas under the peaks yield the absorption strengths for the two transitions; these are transformed into oscillator strengths using the expression²¹

$$f = 1.1296 \times 10^{12} \int \sigma(\hat{\nu}) d\hat{\nu}$$

where $\sigma(\hat{\nu})$ is the absorption cross section ($\text{cm}^2 \text{molecule}^{-1}$) as a function of wavenumber, $\hat{\nu}$. At 296 K, the integrated absorption cross sections are $2.63 \times 10^{-20} \text{ cm}^2 \text{molecule}^{-1} \text{ cm}^{-1}$ for $\nu = 3$ and $2.37 \times 10^{-21} \text{ cm}^2 \text{molecule}^{-1} \text{ cm}^{-1}$ for $\nu = 4$.

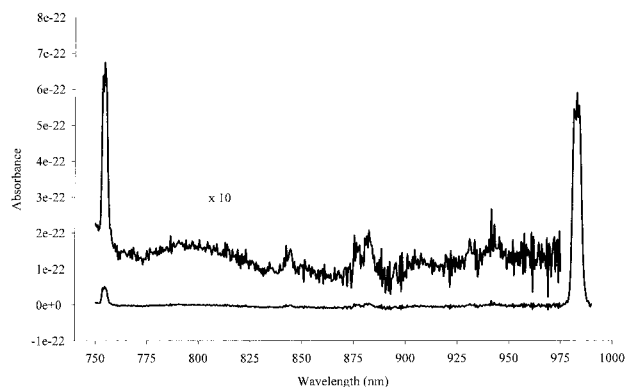


Figure 1. Nitric acid overtone spectrum in the $\nu_{\text{OH}} = 3, 4$ region.

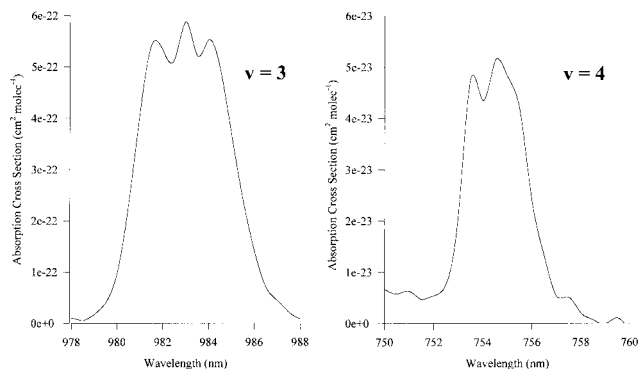


Figure 2. Expanded view of the $\nu_{\text{OH}} = 3$ and $\nu_{\text{OH}} = 4$ regions. The integrated cross sections are $(2.63 \pm 0.26) \times 10^{-20} \text{ cm}^2 \text{ molecule}^{-1} \text{ cm}^{-1}$ for $\nu_{\text{OH}} = 3$ and $(2.37 \pm 0.24) \times 10^{-21} \text{ cm}^2 \text{ molecule}^{-1} \text{ cm}^{-1}$ for $\nu_{\text{OH}} = 4$.

TABLE 2: Ab Initio MP2/6-311+G(d,p) Dipole Moment Derivative Coefficients for the Hydroxy Group in Nitric Acid

μ	x	y	z
$D(\text{\AA}^{-1})$	-0.4767	0	-1.3792
$D(\text{\AA}^{-2})$	0.6094	0	0.1367
$D(\text{\AA}^{-3})$	0.0338	0	0.7385
$D(\text{\AA}^{-4})$	-0.0442	0	0.0343
$D(\text{\AA}^{-5})$	-0.7949	0	-0.6240
$D(\text{\AA}^{-6})$	1.9928	0	1.7573
$D(\text{\AA}^{-7})$	0.8634	0	2.0468

TABLE 3: Observed Peak Positions and Assignments

λ (nm)	wavenumber (cm^{-1})	separation (cm^{-1})	assignment
983	10 173	0	$3\nu_{\text{OH}}$
942	10 616	443	$3\nu_{\text{OH}} + \nu_{\text{torsion}}$
883	11 325	1152	$3\nu_{\text{OH}} + \nu_{\text{bend}}$
877	11 402	1229	
845	11 834	1661	$3\nu_{\text{OH}} + \nu_{\text{N=O}}$
755	13 245	3072	$4\nu_{\text{OH}}$

These correspond to oscillator strengths for the $3\nu_{\text{OH}}$ and $4\nu_{\text{OH}}$ transitions of 2.97×10^{-8} and 2.68×10^{-9} , respectively. The total uncertainties, mainly composed of pressure uncertainties and the observed S/N, are estimated to be 10% on each value.

Table 4 presents the overtone oscillator strengths calculated at various levels of theory. In all the calculations, the oscillator strength decreases by roughly an order of magnitude per ν level, as expected. We take the results at the QCISD/6-31+G(d,p) level and scale them by a factor 1.15, which is the average ratio of the measured to calculated oscillator strengths for the $\nu = 3$ and $\nu = 4$ transitions. This yields predicted oscillator strengths for $\nu = 5$ and $\nu = 6$ of 2.93×10^{-10} and 3.98×10^{-11} ,

TABLE 4: Calculated Overtone Oscillator Strengths of the OH Stretch in Nitric Acid

	$\nu = 2$	$\nu = 3$	$\nu = 4$	$\nu = 5$	$\nu = 6$
HF/6-31G(d)	6.21	3.08	2.09	1.80	1.79
HF/6-31+G(d,p)	5.29	2.44	1.99	2.26	3.01
HF/6-311+G(d,p)	5.13	2.13	1.47	1.40	2.51
HF/6-311+G(3df,3pd)	4.03	1.81	1.44	2.13	2.82
MP2/6-31G(d)	7.87	3.98	2.74	2.40	2.38
MP2/6-31+G(d,p)	6.13	2.75	2.20	2.66	3.64
MP2/6-311+G(d,p)	6.15	2.42	1.56	1.33	2.03
QCISD/6-31G(d)	8.15	3.83	2.49	2.17	2.24
QCISD/6-31+G(d,p)	6.85	2.78	2.14	2.55	3.46
exponent	10^{-7}	10^{-8}	10^{-9}	10^{-10}	10^{-11}

TABLE 5: Integrated Absorption Cross Sections^a

transition	measured	calculated	predicted	from ref 8
$\nu = 3$	2.63×10^{-20}	2.46×10^{-20}	2.83×10^{-20}	
$\nu = 4$	2.37×10^{-21}	1.89×10^{-21}	2.17×10^{-21}	
$\nu = 5$		2.26×10^{-22}	2.60×10^{-22}	1.5×10^{-22}
$\nu = 6$		3.06×10^{-23}	3.52×10^{-23}	1.9×10^{-23}

^aIn $\text{cm}^2 \text{ molecule}^{-1} \text{ cm}^{-1}$.

respectively. The same method of scaling applied to previous results²² at the QCISD level gives predicted $\Delta\nu = 5, 6$ oscillator strengths within 35% of experiment for HCN and within 25% of experiment for CH₄. Transforming these to integrated absorptions yields integrated absorption cross sections of $2.60 \times 10^{-22} \text{ cm}^2 \text{ molecule}^{-1} \text{ cm}^{-1}$ for $\nu = 5$ and $3.52 \times 10^{-23} \text{ cm}^2 \text{ molecule}^{-1} \text{ cm}^{-1}$ for $\nu = 6$. Table 5 gives the measured, calculated and predicted integrated absorption cross sections for $\nu = 3-6$.

In our model study of direct overtone photolysis of nitric acid in the stratosphere,⁸ we approximated the overtone transitions to $\nu = 5$ and $\nu = 6$ by box functions of width 5 nm and height σ to calculate the integrated absorptions. In that work, the peak absorption cross sections were taken from the estimates given by Crim²¹ to be $1 \times 10^{-24} \text{ cm}^2$ for $\nu = 5$ and $1 \times 10^{-25} \text{ cm}^2$ for $\nu = 6$. As shown in Table 5, the integrated absorption values given here are respectively 1.7 and 1.8 times greater than those estimated in ref 8. The model also included a transition to a ($5\nu_{\text{OH}} + \text{torsion}$) level, 500 cm^{-1} from the pure $5\nu_{\text{OH}}$ transition. Although we do observe such a feature (and others) in the $3\nu_{\text{OH}}$ region, it is much weaker relative to the pure $3\nu_{\text{OH}}$ transition than we assumed in the model. Making the reasonable assumption that the relative intensities of these combination bands will not increase around $\nu = 5$, they should contribute less to the overtone-induced photodissociation of HNO₃ than we assumed in our model study. However, the (almost) factor-of-2 increase in both the $\nu = 5$ and $\nu = 6$ absorption strengths over that assumed in ref 8 suggests that overtone-induced production of OH and NO₂ from nitric acid is at least as important a process as suggested there. If the actual OH overtone intensities in pernitric acid are similarly larger than those assumed in ref 8, pernitric acid could be a significant source of OH at dawn and dusk in the lower-mid stratosphere and upper troposphere. We are continuing our work in this area to determine the pernitric acid overtone absorption cross sections.

Conclusions

In this paper we show that a combination of experimental measurements and ab initio calculations can be used to determine accurate absolute absorption cross sections of OH overtone transitions at chemically relevant energies. This approach serves both as a sensitive test of theory and yields

important parameters for inclusion in atmospheric models. We report measured and [calculated] oscillator strengths of $(2.9 \pm 0.3) \times 10^{-8}$ [2.78×10^{-8}] and $(2.7 \pm 0.3) \times 10^{-9}$ [2.14×10^{-9}] respectively for the $\nu = 3$ and $\nu = 4$ OH local mode transitions of HNO₃. We use these results to predict the oscillator strengths for the chemically relevant $\nu = 5$ and $\nu = 6$ transitions to be 2.9×10^{-10} and 4.0×10^{-11} , respectively. The theory and experiment agree quite well—within about 25%. Both the calculated and experimental numbers are larger than those for the generic OH overtone stretch used for this chromophore to date.²¹ Our results imply that solar pumping of vibrational overtones with visible light in the atmosphere could be a significant photoprocess, competing with photodissociation on the excited electronic surfaces accessible in the near-UV.

Acknowledgment. We wish to thank J. A. Phillips for some technical assistance with nitric acid preparation. D.J.D. and B.R.H. thank NSERC for partial support of this work. V.V. thanks NSF for partial support and C.R.C.W. of the University of Colorado for a Fellowship. NCAR is sponsored by the National Science Foundation. The NCAR portion of this work was partially funded by the Upper Atmosphere Research Program of NASA's Mission to Planet Earth.

References and Notes

- (1) Henry, B. R. *Acc. Chem. Res.* **1987**, *20*, 429, 1987; **1977**, *10*, 207.
- (2) Child, M. S. *Acc. Chem. Res.* **1985**, *18*, 45.
- (3) Nesbitt, D. J.; Field, R. W. *J. Phys. Chem.* **1996**, *100*, 12735.
- (4) Crim, F. F. *J. Phys. Chem.* **1996**, *100*, 12725.
- (5) Burberry, M. S.; Morrell, J. A.; Albrecht, A. C.; Swofford, R. L. *J. Chem. Phys.* **1979**, *70*, 5522.
- (6) Lehmann, K. K.; Smith, A. M. *J. Chem. Phys.* **1990**, *93*, 6140.
- (7) Quack, M. *Annu. Rev. Phys. Chem.* **1990**, *41*, 839.
- (8) Donaldson, D. J.; Frost, G. J.; Rosenlof, K. H.; Tuck, A. F.; Vaida, V. *Geophys. Res. Lett.* **1997**, *24*, 2651.
- (9) (a) Sinha, A.; Vander Wal, R. L.; Crim, F. F. *J. Chem. Phys.* **1989**, *91*, 2929. (b) Sinha, A.; Vander Wal, R. L.; Crim, F. F. *J. Chem. Phys.* **1989**, *92*, 401.
- (10) Fleming, P. R.; Mengyang, L.; Rizzo, T. R. *J. Chem. Phys.* **1991**, *94*, 2425.
- (11) Wennberg, P. O.; Cohen, R. C.; Stimpfle, R. M.; Koplow, J. P.; Anderson, J. G.; Salawitch, R. J.; Fahey, D. W.; Woodbridge, E. L.; Keim, E. R.; Gao, R. S.; Webster, C. R.; May, R. D.; Toohey, D. W.; Avallone, L. M.; Proffitt, M. H.; Loewenstein, M.; Podolske, J. R.; Chan, K. R.; Wofsy, S. C. *Science* **1994**, *266*, 398.
- (12) Staffellbach, T. A.; Orlando, J. J.; Tyndall, G. S.; Calvert, J. G. *J. Geophys. Res.* **1995**, *100D*, 14189.
- (13) Tyndall, G. S.; Orlando, J. J.; Cantrell, C. A.; Shetter, R. E.; Calvert, J. G. *J. Phys. Chem.* **1991**, *95*, 4381.
- (14) (a) Kjaergaard, H. G.; Yu, H.; Schattka, B. J.; Henry, B. R.; Tarr, A. W. *J. Chem. Phys.* **1990**, *93*, 6239. (b) Kjaergaard, H. G.; Henry, B. R. *J. Phys. Chem.* **1995**, *99*, 899.
- (15) Atkins, P. W. *Molecular Quantum Mechanics*, 2nd ed.; Oxford University Press: Oxford, 1983.
- (16) *Gaussian 94, Revision D.3*: Frisch, M. J.; Trucks, G. W.; Schlegel, H. B.; Gill, P. M. W.; Johnson, B. G.; Robb, M. A.; Cheeseman, J. R.; Keith, T.; Petersson, G. A.; Montgomery, J. A.; Raghavachari, K.; Al-Laham, M. A.; Zakrzewski, V. G.; Ortiz, J. V.; Foresman, J. B.; Cioslowski, J.; Stefanov, B. B.; Nanayakkara, A.; Challacombe, M.; Peng, C. Y.; Ayala, P. Y.; Chen, W.; Wong, M. W.; Andres, J. L.; Replogle, E. S.; Gomperts, R.; Martin, R. L.; Fox, D. J.; Binkley, J. S.; Defrees, D. J.; Baker, J.; Stewart, J. P.; Head-Gordon, M.; Gonzalez, C.; Pople, J. A. Gaussian, Inc., Pittsburgh, PA, 1995.
- (17) Schneider, W.; Moortgat, G. K.; Tyndall, G. S.; Burrows, J. P. *J. Photochem. Photobiol. A: Chem.* **1987**, *40*, 195.
- (18) McGraw, G. E.; Bernitt, D. L.; Hisatsune, I. C. *J. Chem. Phys.* **1965**, *42*, 237.
- (19) Stern, S. A.; Mullhaupt, J. T.; Kay, W. B. *Chem. Rev.* **1960**, *60*, 185.
- (20) Rizzo, T. R.; Hayden, C. C.; Crim, F. F. *Faraday Discuss. Chem. Soc.* **1983**, *75*, 223.
- (21) Kauzmann, W. *Quantum Chemistry*; Academic Press: New York, 1957.
- (22) Kjaergaard, H. G.; Daub, C. D.; Henry, B. R. *Mol. Phys.* **1997**, *90*, 201.
- (23) Crim, F. F. *Annu. Rev. Phys. Chem.* **1984**, *35*, 657.
- (24) Harmony, M. D.; Laurie, V. W.; Kuckowski, R. L.; Schwendeman, R. H.; Ramsay, D. A.; Lovas, F. J.; Lafferty, W. J.; Maki, A. G. *J. Phys. Chem. Ref. Data* **1979**, *8*, 619.